Nondegenerate and Degenerate Multi-Solitons for the Reverse-Time Nonlocal Nonlinear Schrödinger Model

Jin-Hao Liu(刘金昊)†, Kai-Li Geng(耿凯莉)†, and Chao-Qing Dai(戴朝卿)*

College of Optical, Mechanical and Electrical Engineering, Zhejiang A&F University, Lin'an 311300, China

(Received 14 February 2025; accepted manuscript online 27 February 2025)

We employ the Hirota bilinear method to systematically derive nondegenerate bright one- and two-soliton solutions, along with degenerate bright-dark two- and four-soliton solutions for the reverse-time nonlocal nonlinear Schrödinger equation. Beyond the fundamental nondegenerate one-soliton solution, we have identified and characterized nondegenerate breather bound state solitons, with particular emphasis on their evolution dynamics. Furthermore, we have conducted a comprehensive analysis of the dynamic behavior exhibited by degenerate bright-dark soliton structures. These findings offer potential applications for nondegenerate and degenerate soliton interactions in nonlocal models.

DOI: 10.1088/0256-307X/42/4/040201 CSTR: 32039.14.0256-307X.42.4.040201

1. Introduction. In recent years, local nonlinear wave models, particularly the nonlinear Schrödinger model (NLSM) and its variants, have played a pivotal role in advancing our understanding of localized wave dynamics across diverse physical systems.[1–3] The extensive research on these models has led to the discovery of numerous soliton solutions, with significant applications in areas such as all-optical switching,[4] fiber lasers,[5] and Bose–Einstein condensates.[6] A groundbreaking development occurred when Ablowitz and Musslimani[7] introduced the nonlocal NLSM (NNLSM), which has since garnered substantial attention from both the physics and mathematics communities. The exact solutions of the NNLSM have been rigorously investigated using various analytical and numerical techniques,[8,9] with particular emphasis on the reverse-time NNLSM as a focal point of research.[10–12] Notably, Wu successfully derived degenerate N-soliton solutions and elucidated the dynamic behavior of bright solitons and breather bound state solitons.[10] Ye *et al.* further explored the dynamics and interactions of dark solitons and anti-dark solitons,[11] while Yang *et al.* revealed that higher-order rogue waves exhibit a unique combination of collapsed and non-collapsed peak structures.[12]

Despite these advancements, a critical gap remains in the study of nondegenerate solitons, particularly those exhibiting multi-peak structures, within the framework of the reverse-time NNLSM. In practical physical systems, the energy redistribution resulting from interactions between solitons with multi-peak distributions represents a phenomenon of considerable scientific interest. In coupled models, the assignment of identical wave numbers to different components yields degenerate solitons,[13,14] whereas the introduction of distinct wave numbers leads to nondegenerate solitons.[8,15] Recent studies have reported nondegenerate localized waves and their wave transition dynamics.[16] Multi-peak one-soliton structures, in particular, hold significant promise for the construction of optical logic gates, as they can enhance data-carrying capacity in optical communication systems.[17] Furthermore, the energy conversion characteristics observed during collisions of multi-peak two-soliton offer exciting possibilities for the design of advanced optical devices, including logic gates, lasers, and quantum information processors. In this work, we employ the Hirota bilinear method to systematically construct nondegenerate bright solitons and degenerate bright-dark multi-solitons for the reverse-time NNLSM, addressing this critical gap in the field.

2. Nondegenerate Solitons and Their Dynamics.

2.1. Hirota Form Equation of Reverse-Time NNLSM. We consider the reverse-time NNLSM

$$\mathrm{i}q_{j,t}(x,t)+q_{j,xx}(x,t)+2\Big[\sum_{l=1}^{2}\sigma_l q_l(x,t)q_l^*(x,-t)\Big]q_j(x,t)=0,\quad j=1,2, \tag{1}$$

where the complex functions $q_j(x,\,t)$ $(j=1,\,2)$ are related to x and t, which represent the amplitude of two polarized waves that are the profile of optical solitons. "*" represents complex conjugation, and x, t are the normalized distance and time, respectively. Generally speaking, the values of σ_l, $(l=1,\,2)$ can be divided into three cases: i) when $\sigma_l=1$, $(l=1,\,2)$, Eq. (1) allows bright solitons;[18] ii) when $\sigma_l=-1$, $(l=1,\,2)$, Eq. (1) allows bright-dark and dark-dark solitons;[11] iii) when $\sigma_l=\pm1$, $(l=1,\,2)$, Eq. (1) allows three types of solitons.[11]

However, nondegenerate solitons have not been reported. In order to obtain them, we consider the transformation

$$q_j(x,\,t)=\frac{g^{(j)}(x,\,t)}{f(x,\,t)},\quad q_j^*(x,\,-t)=\frac{g^{(j)^*}(x,\,-t)}{f^*(x,\,-t)}, \tag{2}$$

†These authors contributed equally to this work.

*Corresponding author. Email: dcq424@126.com

© 2025 Chinese Physical Society and IOP Publishing Ltd. All rights, including for text and data mining, AI training, and similar technologies, are reserved.

where $f(x,\,t)$, $f^*(x,\,-t)$, $g^{(j)}(x,\,t)$, $g^{(j)^*}(x,\,-t)$, $(j=1,\,2)$ are the complex function. In this way, the bilinear form of Eq. (1) reads

$$\begin{aligned}&(\mathrm{i}D_t+D_x^2)g^{(j)}(x,\,t)\cdot f(x,\,t)=0,\quad j=1,2,\\&D_x^2 f(x,\,t)\cdot f^*(x,\,-t)=\sum_{l=1}^{2}\sigma_l g^{(l)}(x,\,t)\cdot g^{(l)*}(x,\,-t).\end{aligned}\tag{3}$$

where D_x and D_t are the traditional Hirota bilinear operators.[8]

2.2. Nondegenerate One-Soliton Solutions. We expand the correlation function in Eq. (2) as

$$\begin{aligned}g^{(j)}(x,\,t)&=\sum_{n=1}^{2}g_{2n-1}^{(j)}\chi^{2n-1},\\g^{(j)^*}(x,\,-t)&=\sum_{n=1}^{2}g_{2n-1}^{(j)^*}\chi^{2n-1},\\f(x,\,t)&=1+\sum_{n=1}^{2}f_{2n}\chi^{2n},\\f^*(x,\,-t)&=1+\sum_{n=1}^{2}f_{2n}^*\chi^{2n}.\end{aligned}\tag{4}$$

We define fundamental solitons as: $g_1^{(1)}=\alpha_1\mathrm{e}^{\eta_1}$, $g_1^{(2)}=\alpha_2\mathrm{e}^{\eta_2}$. The amplitude parameters α_j, $(j=1,\,2)$ are arbitrary, and κ_j, $(j=1,\,2)$ are the wave numbers of solitons. The parameter χ in Eq. (4) is a series expansion. Inserting Eq. (4) into Eq. (3), we obtain a set of equations for the target by collecting coefficients of the same power. Finally, exact fundamental soliton solutions read

$$\begin{aligned}q_j(x,\,t)&=\frac{g_1^{(j)}+g_3^{(j)}}{1+f_2+f_4}\\&=\frac{\alpha_j\mathrm{e}^{\eta_j}+A_1^j\mathrm{e}^{\eta_1+\eta_2+\eta_p^*}}{1+B_1^1\mathrm{e}^{\eta_1+\eta_1^*}+B_2^1\mathrm{e}^{\eta_2+\eta_2^*}+C_1^1\mathrm{e}^{\eta_1+\eta_1^*+\eta_2+\eta_2^*}},\end{aligned}\tag{5}$$

where $j,\,p=1,\,2$, $p\neq j$, and parameters A_1^j, B_j^1, C_1^1 are shown in the Appendix A of Supplement Material.

It is worth noting that we introduce a rational transformation (2), which differs from the traditional Hirota method applied under local conditions.[8] The complex conjugations of two components $q_j^*(x,\,-t)=g^{(j)^*}(x,\,-t)/f^*(x,\,-t)$ are carefully considered, and after substituting them into Eq. (1), we obtain the reverse-time nonlocal bilinear Eq. (3). To accommodate the expansion of Eq. (4), we have made corresponding adjustments to the fundamental soliton structure, defining the complex conjugate form of η_j^*, $(j=1,\,2)$ as $\eta_j^*=-\mathrm{i}\kappa_j x+\mathrm{i}\kappa_j^2 t$ in a consistent manner.

The presence of distinct wave numbers in nondegenerate one-soliton solutions enables the emergence of structures beyond single-peak profiles. In our nondegenerate one-soliton solution, we introduce two different wave numbers κ_1, κ_2 for the solitons. By arbitrarily assigning specific values to these parameters κ_1, $\kappa_2(\kappa_1\neq\kappa_2)$, Figs. 1(a) and 1(b) demonstrate that the one-soliton solutions exhibit

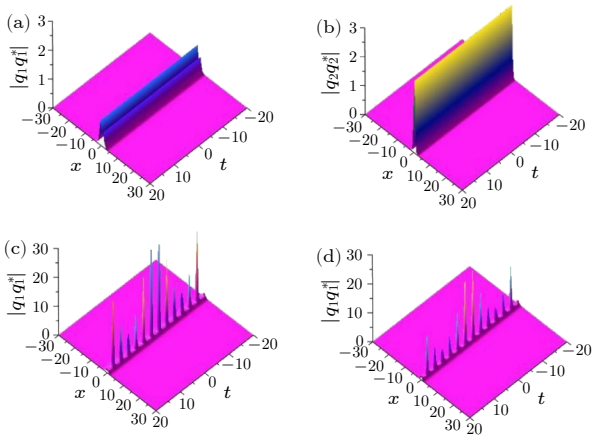

Fig. 1. Quasi-intensity distributions of nondegenerate one-soliton solutions (a, b) and periodical bound solitons (c, d), showing in (a, c) $|q_1q_1^*|$ and (b, d) $|q_2q_2^*|$. Parameters: $\sigma_1=\sigma_2=1$, $\alpha_1=\alpha_2=1+\mathrm{i}$ with (a, b) $\kappa_1=1+\mathrm{i}$, $\kappa_2=2-2\mathrm{i}$, and (c, d) $\kappa_1=1+\mathrm{i}$, $\kappa_2=\mathrm{i}$.

two distinct peaks, confirming their nondegenerate nature. Furthermore, we explore additional soliton structures, particularly bound state solitons. The formation of bound state solitons typically requires that the relative velocity of two bright solitons vanishes.[19] When either the mode resonance condition $\kappa_1=\kappa_2^*$ or the velocity resonance condition $\kappa_1=\kappa_2$ is satisfied, periodic bound state solitons emerge, as illustrated in Figs. 1(c) and 1(d). The imaginary part of the wave numbers governs the parallel propagation and oscillation of these bound state solitons, a finding that aligns with the conclusions established in Ref. [20].

2.3. Nondegenerate Two-Soliton Solutions. To attain the nondegenerate two-soliton solution of the NNLSM, we expand and truncate Eq. (2) as

$$\begin{aligned}g^{(j)}(x,\,t)&=\sum_{n=1}^{4}g_{2n-1}^{(j)}\chi^{2n-1},\\g^{(j)^*}(x,\,-t)&=\sum_{n=1}^{4}g_{2n-1}^{(j)^*}\chi^{2n-1},\\f(x,\,t)&=1+\sum_{n=1}^{4}f_{2n}\chi^{2n},\\f^*(x,\,-t)&=1+\sum_{n=1}^{4}f_{2n}^*\chi^{2n},\quad j=1,2.\end{aligned}\tag{6}$$

We set $g_1^{(1)}=\alpha_{11}\mathrm{e}^{\eta_1}+\alpha_{12}\mathrm{e}^{\eta_2}$, $g_1^{(2)}=\alpha_{21}\mathrm{e}^{\xi_1}+\alpha_{22}\mathrm{e}^{\xi_2}$, $\eta_j=\mathrm{i}\kappa_1^j x+\mathrm{i}(\kappa_1^j)^2 t$, $\xi_j=\mathrm{i}\kappa_2^j x+\mathrm{i}(\kappa_2^j)^2 t$, $(j=1,\,2)$, where the amplitude parameter α_{jp}, $p,\,j=1,\,2$ are arbitrary, and κ_j^p, $j,\,p=1,\,2$ are the wave numbers of the solitons.

The nondegenerate two-soliton solution (6) is

$$q_j(x,\,t)=\frac{g_1^{(j)}+g_3^{(j)}+g_5^{(j)}+g_7^{(j)}}{1+f_2+f_4+f_6+f_8},\quad j=1,2,\tag{7}$$

where the forms of $g_1^{(j)}$, $g_3^{(j)}$, $g_5^{(j)}$, $g_7^{(j)}$, f_2, f_4, f_6, f_8, $D_m^{n(p)}$, E_m^n, $d_m^{n(p)}$, J_{1M2m}^{mn}, j_{1M2m}^{mn}, K_m, L_m, N_m^n, P_m^n, F_{1M2N}^{mn}, F_n, H_{mn}^1, H_{mn}^2, M with $m,\,n,\,p,\,M,\,N=1,\,2$ are given in the Appendix A of Supplement Material.

To verify the existence of nondegenerate solitons in the reverse-time NNLSM, we assign unequal values to the

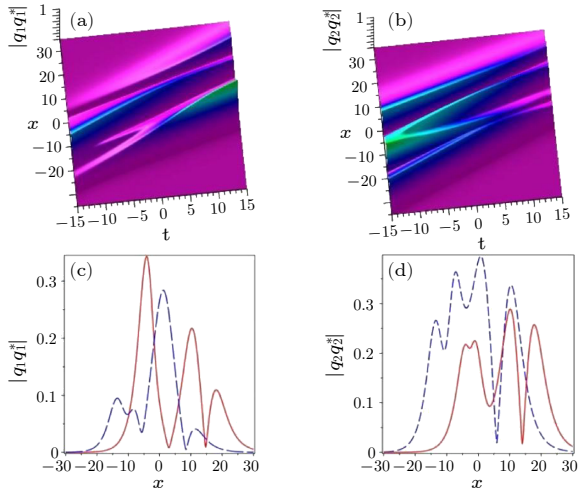

Fig. 2. Quasi-intensity distribution of nondegenerate two-soliton solutions (a, b) with corresponding cross-sections at $t = -5$ (c) and $t = 5$ (d) (Blue and red curves represent the cases before and after the collision) for (a, c) $|q_1 q_1^*|$ and (b, d) $|q_2 q_2^*|$. Parameters: $\sigma_1 = \sigma_2 = 1$, $\kappa_1^1 = 0.5 + 0.2\mathrm{i}$, $\kappa_1^2 = 0.315 - 0.4\mathrm{i}$, $\kappa_2^1 = 0.315 + 0.3\mathrm{i}$, $\kappa_2^2 = 0.5 - 0.4\mathrm{i}$, $\alpha_1^1 = \alpha_1^2 = 0.5 + \mathrm{i}$, $\alpha_2^1 = \alpha_2^2 = 0.55 - \mathrm{i}$.

wave numbers of the solitons. As illustrated in Figs. 2(a) and 2(b), we obtain non-traditional nondegenerate two-soliton interaction profiles. To analyze the energy changes of the solitons more clearly, we have also plotted the intensity profiles at specific instances $t = -5$ and $t = 5$ in Figs. 2(c) and 2(d).

From these figures, it is evident that after the collision, the intensity of solitons in component (q_1) is enhanced, while the intensity in component (q_2) is suppressed. This observation highlights the redistribution of energy between the two components q_1, q_2, while the total energy of the system remains conserved. In the case of degenerate solitons, the polarization vector plays a critical role in altering the shape of solitons during collisions. A similar phenomenon occurs in nondegenerate solitons, where the polarization vector

$$A_j^l = \alpha_{lj} \Big/ \Big(\sum_{k=1}^{2} |\alpha_{kj}|^2 \Big)^{1/2}$$

influences the deformation of soliton profiles. The deformation observed during these collisions suggests that nondegenerate two-soliton in the reverse-time NNLSM cannot stably coexist in communication systems, as their energy redistribution and shape changes may disrupt signal integrity.

3. Degenerate Bright-Dark Even Solitons.

3.1. Hirota Form Equations of Reverse-Time NNLSM. We obtain nonlocal degenerate bright-dark even soliton solutions by the Hirota method.[8] Firstly, we introduce a rational transformation

$$\begin{aligned} q_j(x,t) &= \rho_{j-1} \frac{g^{(j)}(x,t)}{f(x,t)} \mathrm{e}^{\mathrm{i}[\beta_{j-1}x + (2\sigma_2|\rho_1|^2 - \beta_{j-1}^2)t]}, \\ q_j^*(x,-t) &= \rho_{j-1} \frac{g^{(j)^*}(x,-t)}{f^*(x,-t)} \mathrm{e}^{\mathrm{i}[-\beta_{j-1}x + (2\sigma_2|\rho_1|^2 - \beta_{j-1}^2)t]}, \end{aligned} \tag{8}$$

where $f(x,t)$, $f^*(x,-t)$, $g^{(j)}(x,t)$, $g^{(j)^*}(x,-t)$, $(j = 1, 2)$ are all complex functions. $\beta_0 = 0$, $\rho_0 = 1$, ρ_l, β_l $(l = 0, 1, 2)$ are arbitrary constants. The bilinear forms of Eq. (1) are

$$\begin{aligned} &(\mathrm{i}D_t + D_x^2) g^{(1)}(x,t) \cdot f(x,t) = 0, \\ &(\mathrm{i}D_t + D_x^2 + 2\mathrm{i}\beta_1 D_x) g^{(2)}(x,t) \cdot f(x,t) = 0, \\ &(D_x^2 + 2\sigma_2|\rho_1|^2) f(x,t) \cdot f^*(x,-t) \\ &= 2\Big[\sum_{j=1}^{2} \sigma_j |\rho_{j-1}|^2 g^{(j)}(x,t) \cdot g^{(j)^*}(x,-t) \Big]. \end{aligned} \tag{9}$$

3.2. Degenerate Bright-Dark Two-Soliton. Degenerate bright-dark two-soliton reads (8) with

$$g^{(1)} = \begin{vmatrix} \frac{\mathrm{e}^{\eta_1+\eta_1^*}}{k_1^1+k_1^{1*}} & \frac{\mathrm{e}^{\eta_1+\xi_1^*}}{k_1^1+k_2^{1*}} & 1 & 0 & \mathrm{e}^{\eta_1} \\ \frac{\mathrm{e}^{\xi_1+\eta_1^*}}{k_2^1+k_1^{1*}} & \frac{\mathrm{e}^{\xi_1+\xi_1^*}}{k_2^1+k_2^{1*}} & 0 & 1 & \mathrm{e}^{\xi_1} \\ -1 & 0 & G_1 & 0 & 0 \\ 0 & -1 & 0 & G_2 & 0 \\ 0 & -\alpha_1 & -\alpha_2 & 0 & 0 \end{vmatrix}, \quad f = \begin{vmatrix} \frac{\mathrm{e}^{\eta_1+\eta_1^*}}{k_1^1+k_1^{1*}} & \frac{\mathrm{e}^{\eta_1+\xi_1^*}}{k_1^1+k_2^{1*}} & 1 & 0 \\ \frac{\mathrm{e}^{\xi_1+\eta_1^*}}{k_2^1+k_1^{1*}} & \frac{\mathrm{e}^{\xi_1+\xi_1^*}}{k_2^1+k_2^{1*}} & 0 & 1 \\ -1 & 0 & G_1 & 0 \\ 0 & -1 & 0 & G_2 \end{vmatrix},$$

$$g^{(2)} = \begin{vmatrix} \frac{(-k_1^1+\mathrm{i}\beta_1)\mathrm{e}^{\eta_1+\eta_1^*}}{(k_1^1+k_1^{1*})(k_1^{1*}+\mathrm{i}\beta_1)} & \frac{(-k_1^1+\mathrm{i}\beta_1)\mathrm{e}^{\eta_1+\xi_1^*}}{(k_1^1+k_2^{1*})(k_2^{1*}+\mathrm{i}\beta_1)} & 1 & 0 \\ \frac{(-k_2^1+\mathrm{i}\beta_1)\mathrm{e}^{\xi_1+\eta_1^*}}{(k_2^1+k_1^{1*})(k_1^{1*}+\mathrm{i}\beta_1)} & \frac{(-k_2^1+\mathrm{i}\beta_1)\mathrm{e}^{\xi_1+\xi_1^*}}{(k_2^1+k_2^{1*})(k_2^{1*}+\mathrm{i}\beta_1)} & 0 & 1 \\ -1 & 0 & G_1 & 0 \\ 0 & -1 & 0 & G_2 \end{vmatrix},$$

with $G_j = \frac{\sigma_1 \alpha_1 \alpha_1^* (k_j^{1*}+\mathrm{i}\beta_1)(k_j^1-\mathrm{i}\beta_1)}{(k_j^1+k_j^{1*})[(k_j^{1*}+\mathrm{i}\beta_1)(k_j^1-\mathrm{i}\beta_1)+\sigma_2\rho_1\rho_1^*]}$.

To further enrich the soliton dynamics of the reverse-time NNLSM, we present degenerate even bright-dark soliton solutions. Specifically, degenerate bright two-soliton and dark two-soliton solutions are illustrated in Figs. 3(a) and 3(b), respectively. To analyze the soliton interactions in greater detail, we provide sectional diagrams of the soliton collisions in Figs. 3(c) and 3(d), where blue dashed curves represent the solitons before collision and red solid curves depict the solitons after collision. Through our calculations, we determine the strength of the solitons $S_j^- = S_j^+$, $(j = 1, 2)$ with $\mp$ representing the cases before and after collision. This result indicates the existence of elastic collisions between degenerate two-soliton, which implies that degenerate two-soliton of reverse-time NNLSM

can coexist in communication systems.

3.3. Degenerate Bright-Dark Four-Solitons. The four-soliton solutions (8), along with their corresponding parameters, are detailed in Appendix B of the Supplementary Material. The propagation characteristics of the two

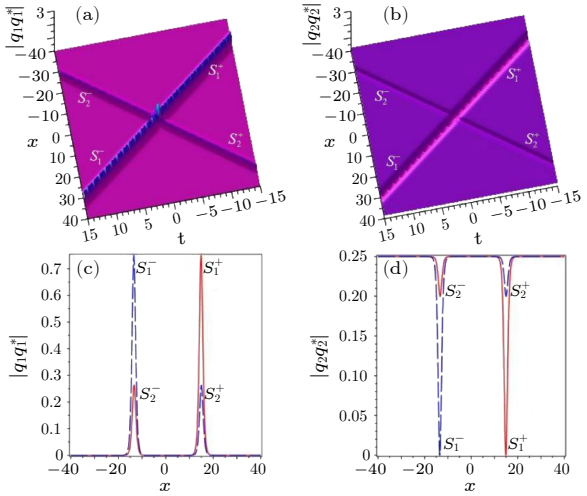

Fig. 3. Quasi-intensity distribution of degenerate bright-dark two-soliton solutions (a, b) with corresponding cross-sectional drawing (c, d) at $t = -5$ (blue curves) and $t = 5$ (red curves): (a, c) $|q_1 q_1^*|$ and (b, d) $|q_2 q_2^*|$. Parameters: $\sigma_1 = 1$, $\sigma_2 = -1$, $\kappa_2^1 = 1 + \mathrm{i}$, $\kappa_2^2 = 1 - \mathrm{i}$, $\alpha_1 = \alpha_2 = 1$, $\sigma_1 = 1$, $\sigma_2 = -1$, $\beta_1 = \beta_2 = 1$, $\rho_1 = 0.5$.

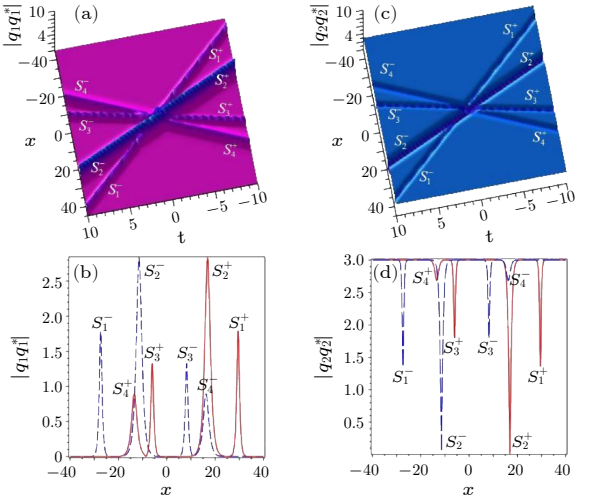

Fig. 4. Quasi-intensity distribution of degenerate bright-dark four-soliton solutions (a, b) with corresponding cross-sectional drawing (c, d) at $t = -5$ (blue curves), $t = 5$ (red curves): (a, c) $|q_1 q_1^*|$ and (b, d) $|q_2 q_2^*|$. Parameters: $\sigma_1 = 1$, $\sigma_2 = -1$, $\kappa_1^1 = 1 + \mathrm{i}$, $\kappa_1^2 = 2 - 0.5\mathrm{i}$, $\kappa_2^1 = 2 + 2\mathrm{i}$, $\kappa_2^2 = 1 - \mathrm{i}$, $\alpha_1^1 = \alpha_1^2 = \alpha_2^1 = \alpha_2^2 = 1$, $\sigma_1 = -1$, $\sigma_2 = -1$, $\rho_1 = 3$, $\beta_1 = \beta_2 = 1$.

components q_1, q_2 are governed by eight arbitrary complex parameters κ_m^n, α_{mn}, $(m, n = 1, 2)$, which determine the shape, amplitude, width, and velocity of the solitons propagating in Kerr media. Specifically, the amplitude of the solitons is controlled by the real part of the wave numbers κ_m^n, $(m, n = 1, 2)$, while their velocity is influenced by the imaginary part of these wave numbers. The shape and width of the solitons are further modulated by the parameters α_{mn}, $(m, n = 1, 2)$. A degenerate bright-dark four-soliton solution is illustrated in Fig. 4. The strength of the solitons, defined as $S_j^- = S_j^+$, $(j = 1, 2, 3, 4)$ with $\mp$ representing the cases before and after the collision. This confirms that the four-solitons undergo elastic collisions in both components, with the strength of the solitons preserved throughout the interaction. Consequently, the system exhibits energy conservation, ensuring that the total energy remains invariant before and after the collisions.

4. Conclusion. In conclusion, we have successfully derived nondegenerate one- and two-soliton solutions, as well as degenerate bright-dark even soliton solutions, for the reverse-time NNLSM using the Hirota bilinear method. For the nondegenerate one-soliton case, by imposing constraints on the relative velocity of solitons, we obtain both traditional two-peak nondegenerate one-solitons and periodic bound state solitons. In the context of nondegenerate two-soliton, we analyze the energy distribution characteristics during their interactions, revealing that while the energy of individual components varies across different scenarios, the total energy of the system remains conserved. To explore the diversity of soliton interactions further, we also derive degenerate bright-dark two-soliton and four-soliton solutions. Our findings demonstrate that these degenerate bright-dark solitons exhibit elastic collision properties, suggesting their potential for stable coexistence in communication systems. Looking ahead, we plan to investigate the phenomena arising from interactions between different types of solitons in greater depth, aiming to uncover novel insights and applications. These efforts will contribute to advancing optical communication technology, and offering new perspectives and strategies for enhancing data transmission and processing capabilities. This work not only expands the theoretical understanding of soliton dynamics in nonlocal systems but also paves the way for practical innovations in photonics and related fields.

Acknowledgements. This work was supported by the National Natural Science Foundation of China (Grant Nos. 12261131495 and 12475008) and the Scientific Research and Developed Fund of Zhejiang A&F University (Grant No. 2021FR0009).

References

[1] Liu X M, Zhang Z Y, and Liu W J 2023 *Chin. Phys. Lett.* **40** 070501
[2] Cao Q H, Geng K L, Zhu B W *et al.* 2023 *Chaos Solitons Fractals* **166** 112895
[3] Yuan W X and Guo R 2024 *Phys. Rev. E* **110** 065307
[4] Si Z Z, Wang Y Y, and Dai C Q 2024 *Sci. Chin. Phys. Mech. Astron.* **67** 274211
[5] Si Z Z, Ju Z T, Ren L F *et al.* 2025 *Laser Photonics Rev.* **19** 2401019
[6] Zhong Y, Triki H, and Zhou Q 2024 *Chin. Phys. Lett.* **41** 070501
[7] Ablowitz M J and Musslimani Z H 2017 *Stud. Appl. Math.* **139** 7
[8] Geng K L, Zhu B W, Cao Q H *et al.* 2023 *Appl. Math. Lett.* **145** 108793

[9] Horikis T P and Ablowitz M J 2017 *Phys. Rev. E* **95** 042211
[10] Wu J P 2021 *Nonlinear Dyn.* **106** 775
[11] Ye R S and Zhang Y 2020 *Stud. Appl. Math.* **145** 197
[12] Yang B and Chen Y 2018 *Chaos* **28** 053104
[13] Feng B F 2014 *J. Phys. A* **47** 355203
[14] Zhu B W, Bo W B, Cao Q H *et al.* 2023 *Chaos* **33** 073132
[15] Stalin S, Ramakrishnan R, and Lakshmanan M 2021 *Photonics* **8** 258
[16] Pan L, Wang L, Liu L, Sun W, and Ren X 2024 *Nonlinearity* **37** 105016
[17] Cai Y J, Wu J W, and Lin J 2022 *Chaos, Solitons & Fractals* **164** 112657
[18] Chen J C and Yan Q X 2020 *Nonlinear Dyn.* **100** 2807
[19] Shi Y, Shen S F, and Zhao S L 2019 *Nonlinear Dyn.* **95** 1257
[20] Stalin S, Senthilvelan M, and Lakshmanan M 2019 *Nonlinear Dyn.* **95** 1767